第 34 卷第 9 期
2018 年 9 月

无 机 化 学 学 报
CHINESE JOURNAL OF INORGANIC CHEMISTRY

Vol.34 No.9
1761-1767

基于β-二酮和四甲基咪唑鎓配体的 Dy(Ⅲ)配合物的合成、结构和磁学性质

葛景园*,[1,2] 陈忠研[2] 马建平[3] 黄 帅[1] 杜 佳[1] 王海欧[1] 苏昆朋[1] 王海英*,[2]

([1]杭州电子科技大学材料与环境工程学院,杭州 310018)

([2]南京大学化学化工学院,配位化学国家重点实验室,南京 210023)

([3]山东师范大学化学化工与材料科学学院,济南 250014)

摘要:利用 2,2,6,6-四甲基庚二酮阴离子(thd^-)和 1,3,4,5-四甲基咪唑鎓阳离子($Tmim^+$)合成了一例单核 Dy(Ⅲ)配合物(Tmim)[Dy(thd)$_4$],通过 X 射线单晶衍射、元素分析等对其进行了结构表征并研究了该配合物的磁学性质。Dy(Ⅲ)中心处于正方反棱柱(D_{4d})的配位环境,其 SAPR-8 参数为 0.316。空间分布中,每个[Dy(thd)$_4$]$^-$阴离子被 $Tmim^+$阳离子有规律地分开,Dy…Dy 最短距离为 1.229 8 nm。磁性研究表明配合物 **1** 具有场诱导的单离子磁体行为,在 500 Oe 直流场下能垒达到 30.9 K。

关键词:配位化学;镝配合物;晶体结构;磁学性质

中图分类号:O614.342 **文献标识码**:A **文章编号**:1001-4861(2018)09-1761-07

DOI:10.11862/CJIC.2018.202

Synthesis, Structure and Magnetic Property of Dysprosium(Ⅲ) Complex Based on β-Diketonate and Tetramethylimidazolium Ligands

GE Jing-Yuan*,[1,2] CHEN Zhong-Yan[2] MA Jian-Ping[3] HUANG Shuai[1]

DU Jia[1] WANG Hai-Ou[1] SU Kun-Peng[1] WANG Hai-Ying*,[2]

([1]*College of Materials and Environmental Engineering, Hangzhou Dianzi University, Hangzhou* 310018, *China*)

([2]*State Key Laboratory of Coordination Chemistry, School of Chemistry and Chemical Engineering, Nanjing University, Nanjing* 210023, *China*)

([3]*School of Chemistry, Chemical Engineering and Materials Science, Shandong Normal University, Jinan* 250014, *China*)

Abstract: A mononuclear dysprosium(Ⅲ) complex, namely (Tmim)[Dy(thd)$_4$] (**1**), was synthesized by the combination of 2,2,6,6-tetramethylheptanedione (thd^-) anion ligand and a 1,3,4,5-tetramethylimidazolium ($Tmim^+$) cation balancing the charge. Complex **1** was structurally and magnetically characterized. The coordination geometry of Dy(Ⅲ) ion is ascribed to approximately square antiprismatic (D_{4d}) symmetry with the SAPR-8 parameter of 0.316. In the solid state, every mononuclear [Dy(thd)$_4$]$^-$ anion is separated by $Tmim^+$ cations regularly and the shortest Dy…Dy distance is 1.229 8 nm. Magnetic studies suggest that complex **1** behaves as a single-ion magnet under 500 Oe dc-applied field with a high effective energy of 30.9 K. CCDC: 1837597.

Keywords: coordination chemistry; dysprosium complexes; crystal structure; magnetic properties

收稿日期:2018-04-17。收修改稿日期:2018-06-07。

国家自然科学基金(No.11604067,11704091),杭州电子科技大学科研启动基金(No.KYS205618010)和南京大学配位化学国家重点实验室开放研究基金(No.SKLCC1810)资助项目。

*通信联系人。E-mail:gejingyuan@hdu.edu.cn

0 Introduction

The coordination complexes consisting of anisotropic metal ions and organic ligands have received considerable research efforts over the past few decades[1-3]. There is a class of materials named as single-molecules magnets (SMMs) that features unique energy barrier and potential applications in quantum computing, high-density information storage, magnetic refrigeration and spintronics devices[4-5]. Since the discovery of single-molecule magnetism in $[TbPc_2]^-$ (Pc=phthalocyanine)[6], a growing number of lanthanide SMMs or lanthanide single-ion magnets (SIMs) have been reported. The advantage is that these types of complexes have large ground-state spin and large intrinsic magnetic anisotropy, especially dysprosium(Ⅲ) complexes[7-8]. Recently, a breakthrough has been made in mononuclear Dy-SMM, $[(Cp^{ttt})_2Dy]^+$ (Cp^{ttt}=1,2,4-tri (tertbutyl)cyclopentadienide), which exhibits magnetic hysteresis at temperatures up to 60 K and a large energy barrier of 1 837 K[9-10]. This result indicates that, with judicious molecular design, magnetic data storage in single molecules at temperatures above the symbolic temperature of 77 K should be possible. However, predicting the properties of lanthanide compounds is still a challenging task. Many researches reveal that the magnetic relaxation behaviors of 4*f*-SMMs/SIMs are particularly sensitive to several factors such as the symmetry-related magnetic anisotropy of individual metal ions, ligand field and intra-/intermolecular magnetic interactio[11-12]. In this regard, continuous efforts should be devoted to synthesize and design new 4*f*-SMMs with diverse structural topologies and to deeply understand the mechanism of relaxation behaviors in SMMs/SIMs.

In addition to improving coordination symmetry to design SMMs with high performance, one of the most compelling trends is that improved properties through targeting the synthesis of structurally simple monometallic SMMs/SIMs rather than polynuclear complexes, and/or diluting diamagnetic species to reduce the molecular interactions. In this paper, we synthesized a new dysprosium(Ⅲ) complex, (Tmim)[Dy(thd)$_4$] (**1**), which contains one mononuclear $[Dy(thd)_4]^-$ anion as a salt of the non-coordinating $Tmim^+$ cation. Complex **1** crystallizes in an orthorhombic *Fdd*2 space group, and an approximately square antiprismatic configuration exists around the Dy(Ⅲ) centre. As expected, every $[Dy(thd)_4]^-$ unit is separated regularly by $Tmim^+$ cation with the shortest Dy…Dy distance of 1.229 8 nm. Both static and dynamic magnetic properties of **1** were also investigated.

1 Experimental

1.1 Chemicals and synthesis

All chemicals and solvents were obtained from the commercial sources and used without further purification. Starting materials, $Dy(thd)_3\cdot 2H_2O$ (Hthd=2,2,6,6-tetramethylheptanedione) and TmimI (1,3,4,5-tetramethylimidazolium iodide) were prepared according to literature methods[13-14]. Complex **1** was synthesized according to the following method: to the ethanol solution of $Dy(thd)_3\cdot 2H_2O$ (500 mg, 0.7 mmol) added 1,3,4,5-tetramethylimidazolium chloride (89 mg, 0.7 mmol) in solid form. The suspension became clear immediately. After stirring for 45 min, the solvent was removed *in vacuo* to obtain a white solid of complex **1**. Suitable single crystals were obtained by the slow evaporation of the resulting solid over the period of three days in their pentane solution. This complex is quite stable in the air, and more importantly, it is very soluble in common organic solvents, such as methanol, ethanol and dichloromethane. Elemental analysis Calcd. for $C_{51}H_{89}DyN_2O_8$(%): C, 60.01; H, 8.79; N, 2.74. Found(%): C, 60.65; H, 8.71; N, 2.85.

1.2 Crystal structure determination

The crystal structures were determined on a Bruker Smart Apex Ⅱ CCD diffractometer (Mo $K\alpha$ radiation, λ=0.071 073 nm). The cell parameters were retrieved and refined by using computer software (SMART and SAINT, respectively)[15]. Corrections for incident and diffracted beam absorption effects were applied using SADABS supplied by Bruker[16]. Both structures were solved and refined against F^2 by the full-matrix least-squares using the SHELXL-97 program[17]. All non-hydrogen atoms were refined with

anisotropic thermal parameters, and hydrogen atoms of the organic ligands and the hydroxide anion were calculated theoretically onto the specific atoms and refined isotropically with fixed thermal factors. A number of restraints were applied owing to disorder in the *p*-*tert*-butyl groups of thd⁻ ligand. Crystal data, data collection parameters, and refinement statistics for complex **1** are given in Table 1. Selected bond distances and bond angles are listed in Table 2.

CCDC: 1837597.

Table 1　Crystal data and structure refinements for 1

Formula	$C_{51}H_{89}DyN_2O_8$	Temperature / K	123(2)
Formula weight	1 020.74	Size / mm	0.16×0.15×0.15
Crystal system	Orthorhombic	*F*(000)	8 624
Space group	*Fdd*2	Absorption coefficient / mm^{-1}	1.314
a / nm	2.573 25(15)	Reflection collected, used	44 728, 6 890
b / nm	3.726 9(2)	Independent reflection (R_{int})	10 803(0.060 2)
c / nm	2.455 77(14)	Goodness-of-fit on F^2	1.029
V / nm^3	23.551(2)	θ range for data collection / (°)	1.92~25.50
Z	16	R_1, wR_2 [$I>2\sigma(I)$]	0.053 9, 0.142 5
D_c / ($g\cdot cm^{-3}$)	1.152		

Table 2　Selected bond lengths (nm) and angles (°) for 1

Dy(1)-O(2)	0.231 3(6)	Dy(1)-O(4)	0.234 2(7)	Dy(1)-O(7)	0.236 4(5)
Dy(1)-O(8)	0.232 1(6)	Dy(1)-O(1)	0.235 6(6)	Dy(1)-O(3)	0.237 3(6)
Dy(1)-O(6)	0.234 0(6)	Dy(1)-O(5)	0.235 9(9)		
O(2)-Dy(1)-O(8)	143.4(2)	O(4)-Dy(1)-O(1)	77.0(3)	O(4)-Dy(1)-O(7)	144.9(2)
O(2)-Dy(1)-O(6)	79.0(2)	O(2)-Dy(1)-O(5)	139.7(2)	O(1)-Dy(1)-O(7)	77.2(2)
O(8)-Dy(1)-O(6)	111.1(3)	O(8)-Dy(1)-O(5)	73.6(3)	O(5)-Dy(1)-O(7)	111.1(3)
O(2)-Dy(1)-O(4)	113.3(3)	O(6)-Dy(1)-O(5)	69.4(2)	O(2)-Dy(1)-O(3)	72.0(2)
O(8)-Dy(1)-O(4)	81.5(3)	O(4)-Dy(1)-O(5)	80.1(3)	O(8)-Dy(1)-O(3)	143.3(3)
O(6)-Dy(1)-O(4)	141.0(3)	O(1)-Dy(1)-O(5)	147.3(3)	O(6)-Dy(1)-O(3)	78.8(2)
O(2)-Dy(1)-O(1)	71.7(2)	O(2)-Dy(1)-O(7)	80.3(2)	O(4)-Dy(1)-O(3)	71.3(2)
O(8)-Dy(1)-O(1)	80.2(3)	O(8)-Dy(1)-O(7)	70.8(2)	O(1)-Dy(1)-O(3)	115.7(3)
O(6)-Dy(1)-O(1)	140.1(2)	O(6)-Dy(1)-O(7)	71.5(2)	O(5)-Dy(1)-O(3)	77.7(3)

1.3　Physical measurements

Elemental analysis was performed on an Elementar Vario MICRO analyzer. The static magnetic susceptibilities for **1** were collected on a Quantum Design MPMS-XL7 SQUID magnetometer in the temperature range of 2~300 K for direct-current (dc) applied fields ranging from 0 to 70 kOe. The alternating current (ac) susceptibilities were obtained using an oscillating field of 5 Oe with the frequency ranging from 1 to 1 488 Hz. All magnetic data were corrected for the sample holder by a previous calibration and for the diamagnetism estimated from Pascals tables[18].

2　Results and discussion

2.1　Crystal structure

The X-ray crystal structure analysis reveals that **1** crystallizes in the orthorhombic space group *Fdd*2. As depicted in Fig.1a, the asymmetric unit contains one mononuclear $[Dy(thd)_4]^-$ anion and one $Tmim^+$ cation. In each $[Dy(thd)_4]^-$ anion, the central Dy(Ⅲ) ion is coordinated by eight O atoms from four thd⁻ ligands to form an octahedral $[DyO_8]$ coordination sphere. The Dy-O bonds range from 0.231 3 to 0.237 3 nm within the normal range according to the previous reports[19]. The coordination environment of Dy(Ⅲ) center was also

confirmed by the continuous shape measures (CShM) values calculated by SHAPE 2.1 software. As shown in Table 3, Dy1 ion lies in a square antiprismatic (D_{4d}) symmetry with a small SAPR-8 value of 0.316. Four O atoms from two thd$^-$ ligands compose an upper (O5, O6, O7 and O8) and a lower (O1, O2, O3 and O4) square planes. The twist angle (φ) between these two planes is 44.12° (Fig.1b), which is very close to that expected for an ideal D_{4d} symmetry (φ=45°). The two planes are in a nearly parallel arrangement with a slight dihedral angle of 0.334°, and the Dy(Ⅲ) ion is unevenly spaced between them with distances of 0.132 8 nm from the upper plane and 0.126 8 nm from the lower plane, respectively.

In the packing motif, [Dy(thd)$_4$]$^-$ units stack together in an ABAB fashion in the *bc* plane (Fig.2a), and each [Dy(thd)$_4$]$^-$ anions is surrounded regularly by the charge balanced Tmim$^+$ cations with the shortest DyN distance of 0.570 1 nm (Fig.2b). The existence of Tmim$^+$ cation makes a larger Dy⋯Dy separated distance (d_{min}=1.229 8 nm). No significant interlayer interactions have been found.

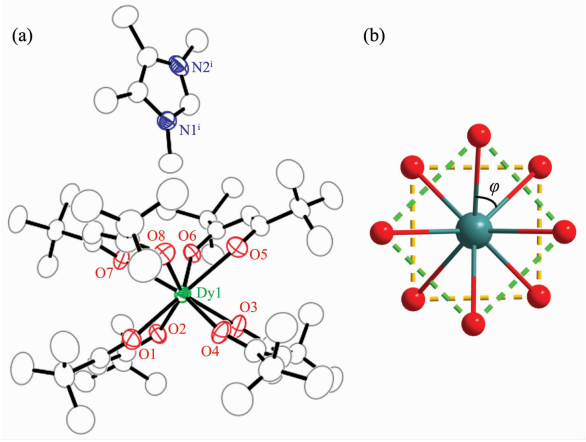

30% probability displacement ellipsoids; All labels of C atoms are omitted for clarity; Symmetry codes: ^{i} x, 1+y, −1+z

Fig.1 (a) Coordination environment around Dy(Ⅲ) ion in complex **1**; (b) Perspective showing the φ structural features

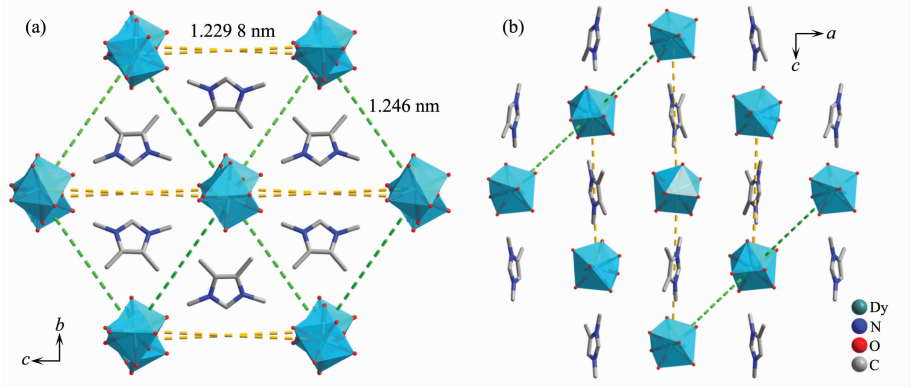

All of C atoms from the thd$^-$ ligands are omitted for clarity

Fig.2 Crystal-packing diagram of **1** in the bc plane (a) and *ac* plane (b)

Table 3 Continuous shape measures calculations (CShM) for 1*

ML8	SAPR-8 (D_{4d})	TDD-8 (D_{2d})	JBTPR-8 (C_{2v})	BTPR-8 (C_{2v})
Dy1	0.316	2.440	2.925	2.382

*SAPR-8: square antiprism; TDD-8: triangular dodecahedron; JBTPR-8: biaugmented trigonal prism J50; BTPR-8: biaugmented trigonal prism

2.2 Magnetic properties

Direct current (dc) magnetic susceptibility data for complex **1** were collected under an applied field of 100 Oe from 2 to 300 K on freshly prepared samples (Fig.3). The room-temperature $\chi_M T$ value of 14.23 cm^3·K·mol^{-1} is in good agreement with the value of one mononuclear Dy(Ⅲ) ion (14.17 cm^3·K·mol^{-1}, J=15/2, g=4/3)[11]. As the temperature decreases, the $\chi_M T$ product decreases slowly and more rapidly below 50 K, which is likely due to the progressive depopulation of the Dy(Ⅲ) excited Stark sublevels and/or the possible antiferromagnetic dipole-dipole interaction between

the molecules[21]. At low temperature, the $\chi_M T$ value remains almost unchanged at 11.23 $cm^3 \cdot K \cdot mol^{-1}$, suggesting negligible magnetic interactions[21]. The field-dependent magnetization of **1** from zero to 70 kOe dc field at 2, 3, 5 and 8 K is shown in Fig.3 inset in the form of M versus H. The curve shows a rapid increase before 10 kOe and then a more gradual increase to 5.59$N\beta$ at 2 K and 70 kOe without saturation, which can be attributed to the presence of crystal-field effects and the low-lying excited states[11]. This is also supported by the non-superposition of isotemperature lines in the M versus H/T curves (Fig.4).

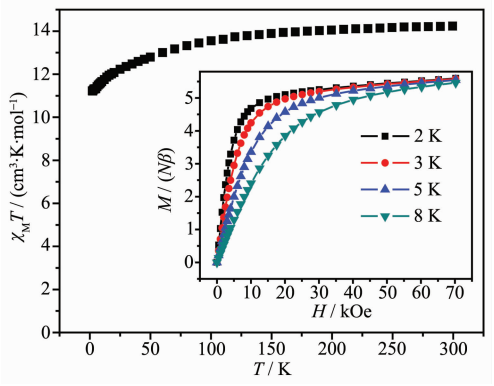

Inset: Field-dependent magnetizations for **1** at the indicated temperatures

Fig.3　Temperature dependence of $\chi_M T$ for complex **1** at 100 Oe field

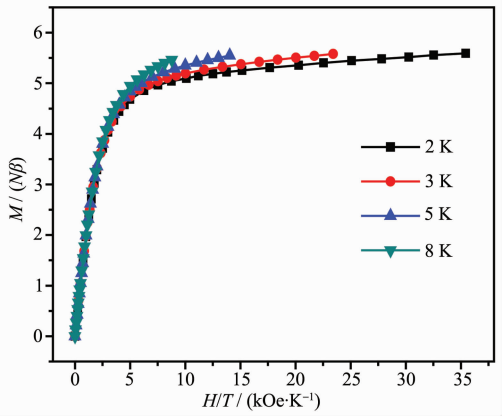

Fig.4　Experimental M versus H/T plots at different temperatures for complex **1**

The alternating current (ac) magnetic susceptibilities were measured to detect the magnetic dynamic behavior of complex **1**. The temperature-dependent ac susceptibility measurements under zero dc-applied field in the frequency range of 1~1 488 Hz are depicted in Fig.5, showing obvious in-phase signals (χ') and out-of-phase signals (χ''). The obvious "tails" of the χ'' signal at temperatures down to 10 K reveal the slow relaxation of magnetization, but no peaks were observed even at a low temperature of 1.8 K and high frequency of 1 488 Hz. The absence of peak maxima in χ'' siganls is mostly resulted from the quantum tunneling of magnetization (QTM) process, which is often revealed in 4*f*-based SMMs[11]. The energy barrier or characteristic relation time of **1** cannot be obtained according to the Arrhenius law: $\tau = \tau_0 \exp[(\Delta E/(k_B T)]$. However, fitting to $\ln(\chi''/\chi') = \ln(\omega\tau_0) + E_a/(k_B T)$ (ω: oscillating frequency of the ac experiment, τ_0: pre-exponential factor of Arrhenius law, E_a: energy barrier, k_B: Boltzmann constant)[22] allows us to roughly evaluate the energy barrier E_a/k_B of 0.51 K (Fig.6).

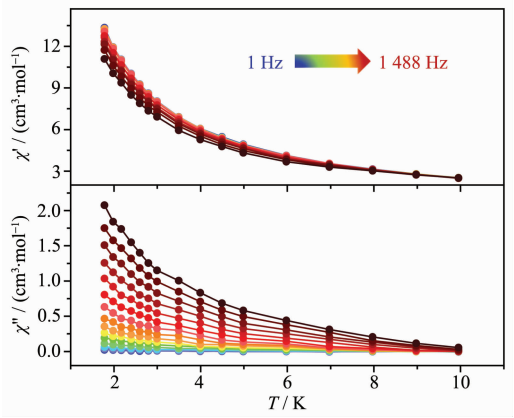

Fig.5　Temperature-dependent in-phase (χ') and out-of-phase signals (χ'') ac susceptibility signals at different frequencies in a 5 Oe ac field oscillating at 1~1 488 Hz under zero dc field for **1**

When a 500 Oe external field was introduced, the well-shaped peaks of χ'' are fully observed(Fig.7). It is worth noting that the χ'' signal at low temperature shows an increase trend with the cooling of temperature, indicating the existence of the other relaxation pathways. This type of multiple relaxation processes is not unusual in mononuclear SMMs/SIMs examples, which may be attributed to the intermolecular interactions or the different conformers of molecule resulting from the ligand disorder[21,23]. The above result confirms the field-induced single-ion magnetic behavior of **1**. Arrhenius law was allowed to

afford the energy barrier E_a/k_B of 30.9 K and the pre-exponential factor $\tau_0=6.47\times10^{-7}$ s (R=0.995 7) (Fig.8).

The Dy(Ⅲ) ion in complex **1** locates in a high D_{4d} symmetry with the small SAPR-8 value of 0.316. Herein, the larger SAPR-8 parameters, the greater the deviation from an ideal D_{4d} symmetry. One [DyO_8] family member [Hex_4N][Dy(DBM)$_4$] (DBM=dibenzoylmethane; Hex_4N^+=tetrahexylammonium) with the more perfect square antiprismatic geometry of Dy(Ⅲ) center has been reported, in which the χ'' peaks under zero dc field can only be observed at frequencies higher than 3 160 Hz[21]. Comparing **1** with [Hex_4N][Dy(DBM)$_4$], the dynamic magnetic behaviors for 4*f*-based SMMs/SIMs are affected not only by the coordination geometry of central metal core, but also by several other factors such as the ligand field, magnetic anisotropy, magnetic interactions and multiple relaxation pathways[20]. Yet further studies are required to determine exactly the relaxation mechanisms in this type of systems.

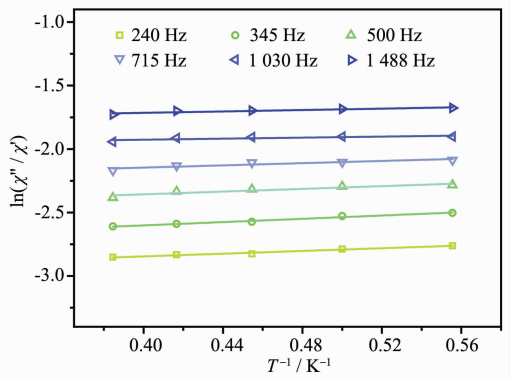

Solid lines represent the best fittings

Fig.6 Plots of ln(χ''/χ') versus T^{-1} for **1** under zero dc field

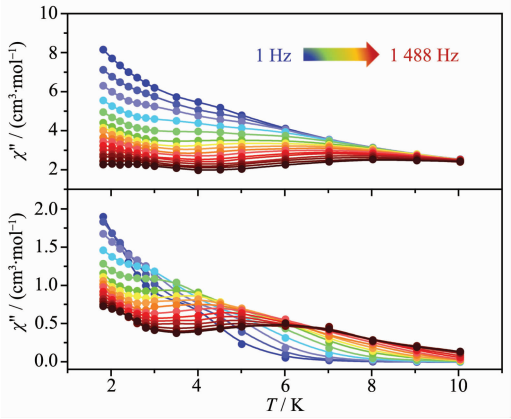

Fig.7 Temperature-dependent in-phase (χ') and out-of-phase signals (χ'') ac susceptibility signals at different frequencies in a 5 Oe ac field oscillating at 1~1 488 Hz under 500 Oe dc field for **1**

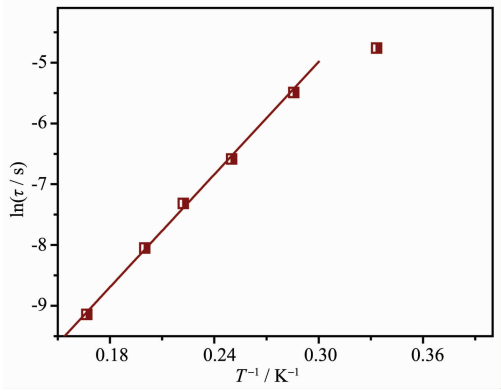

Fig.8 Arrhenius fitting for lnτ vs T^{-1} plot of **1** under 500 Oe dc field

3 Conclusions

In summary, a new dysprosium (Ⅲ) complex (Tmim)[Dy(thd)$_4$] (**1**) was synthesized and structurally characterized. Dy (Ⅲ) centre locates in an approximately ideal square antiprismatic geometry. The [Dy(thd)$_4$]$^-$ anions are separated regularly by $Tmim^+$ cations with the shortest Dy⋯Dy distance of 1.229 8 nm, suggesting that the incorporation of diamagnetic species into molecule magnets can be useful for minimizing intermolecular interactions between spin centers. Moreover, complex **1** exhibits a field-induced single-ion magnetic behavior with a high effective energy of 30.9 K. Taking the advantages of good solubility and the magnetic behavior, **1** will have possible application in the preparation of organic films with slow magnetic relaxation. Further investigations to obtain new molecular architectures by choosing appropriate organic ligands to link paramagnetic metal ions together are underway in our laboratory.

References:

[1] Sessoli R, Tsai H L, Schake A R, et al. *J. Am. Chem. Soc.*, **1993**,**115**(5):1804-1816

[2] Wu X W, Pan F, Zhang D, et al. *CrystEngComm*, **2017**,**19**(39):5864-5872

[3] YU Qin(余沁), WANG Da-Peng(王大鹏), MA Jian-Ping(马建平), et al. *Chinese J. Inorg. Chem.*(无机化学学报), **2017**,

33(12):2345-2350

[4] Vincent R, Klyatskaya S, Ruben M, et al. *Nature*, **2012**,**488**: 357-360

[5] Aulakh D, Pyser J B, Zhang X, et al. *J. Am. Chem. Soc.*, **2015**,**137**(29):9254-9257

[6] Ishikawa N, Sugita M, Ishikawa T, et al. *J. Am. Chem. Soc.*, **2003**,**125**(29):8694-8695

[7] Woodruff D N, Winpenny R E, Layfield R A. *Chem. Rev.*, **2013**,**113**(7):5110-5148

[8] Katoh K, Umetsu K, Breedlove B K, et al. *Sci. China Chem.*, **2012**,**55**(6):918-925

[9] Goodwin C A P, Ortu F, Reta D, et al. *Nature*, **2017**,**548**: 439-442

[10]Guo F S, Day B M, Chen Y C, et al. *Angew. Chem. Int. Ed.*, **2017**,**56**(38):11445-11449

[11]Ge J Y, Wang H Y, Su J, et al. *Inorg. Chem.*, **2018**,**57**(3): 1408-1416

[12]Zhang L, Zhang Y Q, Zhang P, et al. *Inorg. Chem.*, **2017**,**56** (14):7882-7889

[13]Eisentraut K J, Sievers R E, Coucouvanis D, et al. *Inorg. Synth.*, **2007**,**11**:94-98

[14]Blümel M, Crocker R D, Harper J B, et al. *Chem. Commun.*, **2016**,**52**(51):7958-7961

[15]*SAINT-Plus, Version* 6.02, Bruker Analytical X-ray System, Madison, WI, **1999**.

[16]Sheldrick G M. *SADABS, An Empirical Absorption Correction Program*, Bruker Analytical X-ray Systems, Madison, WI, **1996**.

[17]Sheldrick G M. *SHELXTL*-97, *Program of Crystal Struture Refinement*, University of Göttingen, Germany, **1997**.

[18]Li J, Han Y, Cao F, et al. *Dalton Trans.*, **2016**,**45**(22):9279-9284

[19]HU Peng(胡鹏), XIAO Feng-Ping(肖凤屏), ZHI Zhong-Qiang(植中强), et al. *Chinese J. Inorg. Chem.*(无机化学学报), **2017**,**33**(7):1273-1279

[20]Ge J Y, Ru J, Gao F, et al. *Dalton Trans.*, **2015**,**44**(35):15481-15490

[21]Sun W B, Yan B, Zhang Y Q, et al. *Inorg. Chem. Front.*, **2014**,**1**(6):503-509

[22]Langley S K, Moubaraki B, Murray K S. *Inorg. Chem.*, **2012**, **51**(7):3947-3949

[23]Fortea-Pérez F R, Vallejo J, Julve M, et al. *Inorg. Chem.*, **2013**,**52**(9):4777-4779